VIROLOGY 228, 229–235 (1997)
ARTICLE NO. VY968392

Structure of the Herpes Simplex Virus Capsid: Peptide A862-H880 of the Major Capsid Protein Is Displayed on the Rim of the Capsomer Protrusions

JULIET V. SPENCER,* BENES L. TRUS,†,‡ FRANK P. BOOY,‡ ALASDAIR C. STEVEN,‡ WILLIAM W. NEWCOMB,* and JAY C. BROWN*,[1]

*Department of Microbiology and Cancer Center, University of Virginia Health Sciences Center, Charlottesville, Virginia 22908; †Laboratory of Structural Biology, National Institute of Arthritis, Musculoskeletal and Skin Diseases, National Institutes of Health, Bethesda, Maryland 20892; and ‡Computational Bioscience and Engineering Laboratory, Division of Computer Research and Technology, National Institutes of Health, Bethesda, Maryland 20892

Received October 8, 1996; returned to author for revision November 13, 1996; accepted December 5, 1996

The herpes simplex virus-1 (HSV-1) capsid shell has 162 capsomers arranged on a $T = 16$ icosahedral lattice. The major capsid protein, VP5 (MW = 149,075) is the structural component of the capsomers. VP5 is an unusually large viral capsid protein and has been shown to consist of multiple domains. To study the conformation of VP5 as it is folded into capsid protomers, we identified the sequence recognized by a VP5-specific monoclonal antibody and localized the epitope on the capsid surface by cryoelectron microscopy and image reconstruction. The epitope of mAb 6F10 was mapped to residues 862–880 by immunoblotting experiments performed with (1) proteolytic fragments of VP5, (2) GST-fusion proteins containing VP5 domains, and (3) synthetic VP5 peptides. As visualized in a three-dimensional density map of 6F10-precipitated capsids, the antibody was found to bind at sites on the outer surface of the capsid just inside the openings of the *trans*-capsomeric channels. We conclude that these sites are occupied by peptide 862–880 in the mature HSV-1 capsid.

INTRODUCTION

Herpes simplex virus-1 is widespread in the population, with primary infection causing recurrent fever blisters. Infrequently, HSV infections cause severe disorders including retinitis and encephalitis. Immunocompromised patients, such as those undergoing chemotherapy or receiving organ transplants, are at particular risk of developing life-threatening complications due to reactivation of latent herpesvirus infections.

In structure, HSV-1 is representative of members of the herpesvirus family. The virion consists of an external membrane envelope, a proteinaceous layer called the tegument, and an icosahedral capsid containing the double-stranded linear DNA genome (Roizman, 1986; Schrag *et al.,* 1989). When the nuclei of HSV-1-infected cells are disrupted, three capsid species, called A-capsids, B-capsids, and C-capsids, can be isolated by sedimentation on a sucrose gradient (Gibson and Roizman, 1972; Perdue *et al.,* 1975). A-capsids are empty and considered to result from abortive DNA packaging. B-capsids contain a core of scaffolding protein, while C-capsids are fully packaged with the DNA genome and mature into infectious virions. The capsid shell, which is 125 nm in diameter and approximately 15 nm thick, is common to all three types of capsid. The major structural features of the capsid shell are 162 capsomers which lie on a $T = 16$ icosahedral lattice (Baker *et al.,* 1990; Newcomb *et al.,* 1993). Of the 162 capsomers, 150 are hexons that form the faces and edges of the icosahedral capsid, while one penton is found at each of the twelve vertices. The major capsid protein, VP5 (MW 149,075; coded by the UL19 gene) is the structural subunit of the hexons and the pentons; hexons are VP5 hexamers, while pentons are VP5 pentamers (Newcomb *et al.,* 1993; Trus *et al.,* 1992). In addition to the capsomers, the capsid shell contains a total of 320 trivalent structures called triplexes (Newcomb *et al.,* 1993; Zhou *et al.,* 1994). The triplexes lie above the capsid floor connecting capsomers in groups of three. Triplexes may vary in composition, but on average they are heterotrimers, composed of one copy of VP19C (MW 50,260; UL38 gene) and two copies of VP23 (MW 34,268; UL18 gene). Six copies of VP26 (MW 12,095; UL35 gene) are located on the outer rim of each hexon where they appear as horn-shaped protrusions (Booy *et al.,* 1994; Trus *et al.,* 1995; Zhou *et al.,* 1995).

The structure of the capsomers is most clearly defined in three-dimensional reconstructions of the HSV-1 capsid computed to 1.9- to 3.0-nm resolution from electron micrographs of capsids preserved in the frozen-hydrated state (Booy *et al.,* 1994; Newcomb *et al.,* 1993; Trus *et al.,* 1995; Zhou *et al.,* 1994, 1995). In such reconstructions, the hexon protrusions can be seen to be cylindrical projections with a height of 11 nm and a diameter of 17 nm. Each hexon is traversed by an axial channel with a diameter of 5 nm at the external surface. The VP5 subunits of each hexon appear to have three distinct domains; a diamond-shaped upper domain, a stem-like

[1] To whom correspondence and reprint requests should be addressed. Fax: (804) 982-1071. E-mail: jcb2g@virginia.edu.

0042-6822/97 $25.00

central domain, and a basal domain. The penton subunits are structurally similar to the hexon subunits despite their difference in rotational symmetry. The lower domains of both hexons and pentons interact to form the thin (3–4 nm) capsid floor.

Although the location of each capsid protein is now known, we are still lacking the information required to understand molecular interactions among them. Monoclonal antibodies (mAbs) can be used to clarify capsid structure by enhancing information obtained by electron microscopy and image reconstruction techniques (Francis *et al.,* 1992; Olson *et al.,* 1991; Smith *et al.,* 1993; Trus *et al.,* 1992). By identifying the epitope of a specific mAb with immunochemical methods, the antibody binding site observed with structural methods can be presumed to be the location of the amino acid residues recognized by the antibody. Here we present the coordinated application of cryoelectron microscopy, three-dimensional image reconstruction, and epitope mapping of a VP5-specific mAb to examine capsomer conformation. We describe for the first time an amino acid sequence that correlates to a known morphological binding site on the HSV-1 capsid.

MATERIALS AND METHODS

Virus growth and capsid purification

The 17MP strain of HSV-1 was grown in monolayer cultures of BHK-21 cells. B-capsids were purified from infected cells by the method of Perdue *et al.* (1975). Briefly, cells were disrupted by sonication in the presence of 1% Triton X-100, and capsids were banded on a 20–50% sucrose gradient (Newcomb and Brown, 1991). Purified B-capsids were then extracted with 2.0 *M* guanidine hydrochloride to obtain G-capsids as described by Newcomb and Brown (1991). G-capsids were recovered by centrifugation through a 150-μl layer of 25% sucrose for 1 hr at 22,000 rpm in a Beckman SW50.1 rotor at 4°. Extracted capsids were resuspended in TNE buffer at a concentration of 1 mg/ml for electron microscopy and SDS–PAGE analysis.

Monoclonal antibody 6F10

Monoclonal antibody 6F10 was produced from a cloned hybridoma cell line as described by Newcomb *et al.* (1996). MAb 6F10 was found to precipitate HSV-1 capsids and recognize VP5 specifically in an immunoblot.

Cryoelectron microscopy

Capsid preparations to be examined by cryoelectron microscopy were suspended in PBS at a concentration of approximately 0.5 mg/ml. G-capsids (1 mg/ml in PBS) were mixed with 1/10 vol mAb 6F10 (4 mg/ml) in a total reaction volume of 50 μl at room temperature. The immunoprecipitate settled out of solution and the supernatant was decanted. The precipitate was then resuspended in 100 μl PBS and dispersed by sonication. Thin films of control capsid suspensions or immunoprecipates were rapidly frozen in a Reichert KF-80 cryostation and observed as described by Baker *et al.* (1990) with a Phillips EM400T electron microscope equipped with a Gatan model 626 cryoholder.

Image processing and reconstruction

Micrographs recorded at 36,000X were digitized on a Perkin–Elmer 1010MG microdensitometer at a sampling rate corresponding to 0.8 nm per pixel. The unlabeled G-capsid reconstruction was computed previously from 75 images (Booy *et al.,* 1994). The PFT algorithm was used in this study to refine the image to 3.0 nm resolution (Baker and Cheng, 1996). The reconstruction of unlabeled capsids was used as a model for icosahedral reconstructions of mAb 6F10-precipitated capsids, which were calculated to 3.0 nm resolution based on data from 33 particles.

Proteolysis and protein sequencing

G-capsids were fragmented by proteolysis and segments were assayed for antibody binding. Ten micrograms of G-capsids were combined with 10 μg trypsin in a total reaction volume of 20 μl and incubated at 37° for 15 hr. Proteolytic fragments were separated on a 12% SDS–polyacrylamide gel and immunoblotted as described below. Chemiluminescent bands were visualized by exposure to Kodak X-OMAT AR film (Eastman Kodak Company, Rochester, NY). The exposed film was then overlaid onto an identical unprobed Immobilon membrane and reactive bands were marked for excision. Protein sequencing of excised membranes was performed by automated Edman degradation with the 470A Sequenator (Applied Biosystems, Inc., Foster City, CA).

Immunoblotting

Proteins separated by SDS–PAGE were electrophoretically transferred to an Immobilon membrane (Millipore, Medford, MA). Proteins were visualized by staining with 1% Ponceau red in PBS + 1% acetic acid. The membrane was rinsed with dH_20 and blocked overnight at 4° in PBS containing 5% milk and 1% Tween. The membrane was incubated with mAb 6F10 (1:5000 dilution in PBS + 0.5% milk) for 1 hr at room temperature. After washing with PBS + 1% Tween, bound antibodies were detected with peroxidase-conjugated goat anti-mouse immunoglobulins and the ECL Chemiluminescence system (Amersham, Arlington Heights, IL). Membranes were exposed to Kodak X-OMAT AR film.

Construction and expression of recombinant GST-fusion proteins

Fragments of the UL19 gene were amplified using the polymerase chain reaction and subcloned into the

pGEX2T vector (Pharmacia Biotech, Milwaukee, WI) for expression in bacteria. Upstream oligonucleotide primers that encoded the amino-terminal end of the fragment contained a *Bam*HI site followed by UL19 sequences. Downstream oligonucleotide primers that were complementary to the coding strand contained an *Eco*RI site. PCR products were cleaved with *Bam*HI and *Eco*RI, gel purified, and ligated to pGEX2T that had been digested with the same enzymes. The plasmid was transformed into JM109 high efficiency competent cells (Promega, Madison, WI). Protein expression was induced by the addition of IPTG to a final concentration of 1.5 m*M* when bacterial cultures reached an OD_{660} of 0.4. Whole cell lysates were analyzed by SDS–PAGE and immunoblot as described above.

Synthetic peptides

Synthetic 18–19 mers each with a 3–4 amino acid overlap were synthesized with an automated peptide synthesizer (model AMS422, Gilson Medical Electronics, Inc.) using fluorenyl-methoxycarbonyl (Fmoc) chemistry. Peptides were cleaved from resins using TFA/ethandithiol/thioanisole/anisole (90:3:5:2, vol/vol) and purified by HPLC on a C18 reverse phase column. Each peptide was dissolved in ddH_20 as a 1 m*M* solution. Twenty-five-microliter aliquots of each peptide were adsorbed to a nitrocellulose membrane (Schleicher & Schuell, Keene, NH) using a slot blot apparatus (Hoefer Scientific Instruments, San Francisco, CA) and immunoblotted as described above.

RESULTS

Identification of the morphological binding site of mAb 6F10 on HSV-1 G-capsids

To observe binding of mAb 6F10 to the HSV-1 capsid, B-capsids were purified from infected BHK-21 cells by sonication and sedimentation on a sucrose gradient. Purified B-capsids were then extracted with 2.0 *M* guanidine hydrochloride to generate G-capsids, which resemble B-capsids in structure and composition, except that they lack the pentons, peripentonal triplexes, scaffolding protein, and VP26 found in B-capsids.

G-capsids were mixed with mAb 6F10, and the precipitate was viewed by cryoelectron microscopy (Fig. 1b). To confirm the specificity of this reaction, G-capsids were also combined with the VP22a-specific monoclonal antibody MCA406 (Serotec, Washington, DC), but no precipitate was observed. The morphology of the mAb 6F10-precipitated capsids is best appreciated by comparison with control capsids lacking antibody (Fig. 1a). Immunoprecipitated capsids were found to be similar in morphology to control capsids, but at the capsomer surface they showed additional density that we attribute to the presence of mAb 6F10. The control capsids were highly uniform overall in shape and diameter, in contrast to antibody precipitated capsids which were aggregated and appeared slightly larger in diameter than the control capsids (Fig. 1b). The capsomers of immunoprecipitated capsids were found to be more pronounced (arrows in Fig. 1b), probably due to the presence of bound immunoglobulins which project radially outward from the capsomers. SDS–PAGE analysis of precipitated capsids followed by quantitation using the method of Trus *et al.* (1992) indicated that approximately 42% of the potential 6F10 binding sites on the capsid were occupied by bound antibody (data not shown). Thus, only two or three of the six VP5 molecules in each hexon have bound antibody attached.

The binding of mAb 6F10 was examined in greater detail with three-dimensional image reconstructions computed from the cryoelectron micrographs. The surface view and central thin section of the G-capsid reconstruction, as shown in Figs. 1c and 1e, illustrate the size and shape of the hexons. In comparison, the reconstruction of antibody-precipitated capsids shows hexon decoration by mAb 6F10 in the form of a cylindrical extension from the protruding capsomer domain (Fig. 1d). The *trans*-capsomeric channel, clearly visible in the control capsid reconstruction, is entirely occluded by bound antibody. The central thin section further illustrates the significant increase in mass density, which projects 3–4 nm radially outward from the capsomer tips (arrows in Fig. 1f). This increase in density is believed to correspond to bound IgG molecules, indicating that the antibody binding site is at or near the rim of the *trans*-capsomeric channel.

Localization of the epitope to the C-terminal domain of VP5

A rough approximation of the location of the antibody binding sequence was obtained by reaction of mAb 6F10 with VP5 fragments derived from a tryptic digest of HSV-1 G-capsids. Figure 2a shows three major peptide species (approximately 85, 65, and 50 kDa) and several minor peptides which resulted from trypsin treatment of G-capsids. In contrast, the untreated G-capsid control showed the expected three bands corresponding to VP5, VP19C, and VP23 (Newcomb and Brown, 1991). The 150 kDa VP5 band, present in the control HSV G-capsid, was greatly reduced in the trypsin-treated capsid. Two of the major product bands, one migrating at approximately 85 kDa and the other at 65 kDa, may have resulted from a prominently exposed trypsin cleavage site which caused each VP5 molecule to be cleaved into the two large fragments (Steven *et al.,* 1986). Because only one of the two fragments reacted with mAb 6F10, it seems likely that together they represent the full-length VP5 molecule. The other major product band (approximately 50 kDa), which did not react with the antibody, probably results from a combination of the VP19C band and further proteolytic products derived from the 85 kDa fragment of VP5.

Polypeptide fragments from a duplicate gel were elec-

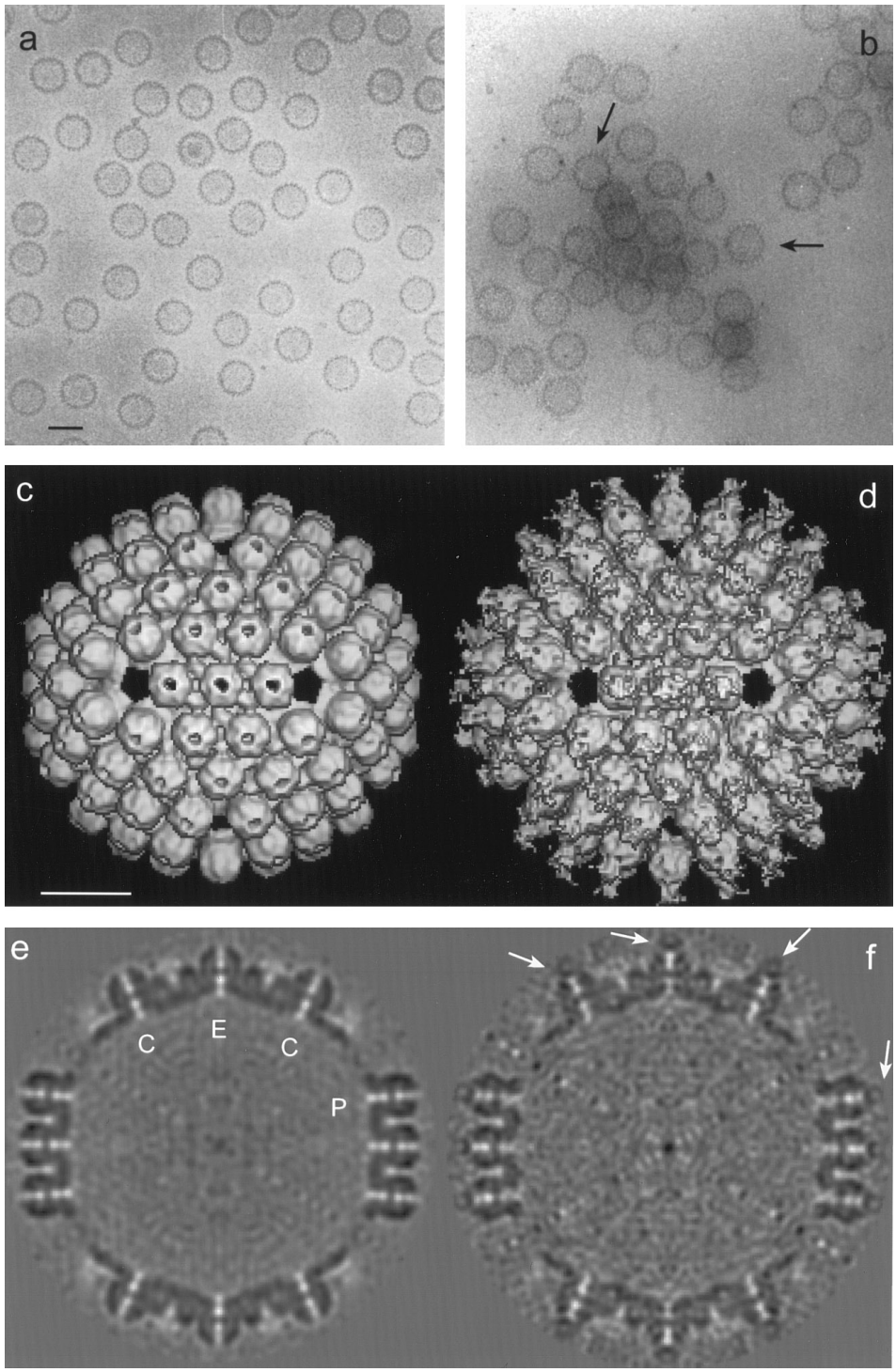

FIG. 1. Cryoelectron micrographs of HSV-1 G-capsids (a) or G-capsids immunoprecipitated with mAb 6F10 (b). Arrows illustrate capsomers which appear larger and more distinct than those in control capsids, possibly due to the presence of bound antibody. Bar, 100 nm. Three-dimensional image reconstructions were computed from digitized micrographs. The reconstruction of unlabeled G-capsids (c, e) was refined to 3.0 nm and used as a model for the PFT algorithm to perform icosahedral reconstructions of mAb 6F10-precipitated capsids (d, f). Reconstructions are presented as viewed along the twofold axis of rotational symmetry. Surface-shaded views are shown in c and d while central thin sections are shown in e and f. Hexons are labeled to indicate central (C), edge (E), or peripentonal (P) hexons. Arrows illustrate the extension of each hexon where antibody is bound. Bar, 25 nm.

trophoretically transferred to an Immobilon membrane and assayed for antibody binding. The results showed that the antibody was bound specifically to two faint bands near the top of the membrane, the 65 kDa fragment and several smaller peptides (Fig. 2b). The identity of the immunoreactive peptides was determined by N-

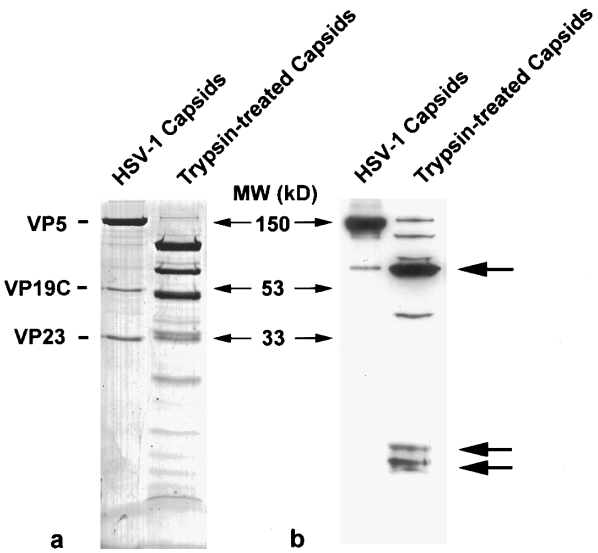

FIG. 2. SDS–PAGE and immunoblot analysis of full-length VP5 and tryptic fragments of VP5. The protein components of purified G-capsids (5 μg total protein) or trypsin-treated G-capsids (10 μg total protein) were separated on a 12% SDS–polyacrylamide gel. Proteins were visualized by Coomassie staining (a). A duplicate, unstained gel was electrophoretically transferred to an Immobilon membrane, and the blot was probed with mAb 6F10 (b). The large arrows on the right indicate proteolytic fragments that were further analyzed by protein sequencing.

terminal protein sequencing. Arrows in Fig. 2 indicate bands that were excised from a duplicate, unprobed membrane by overlaying and aligning the exposed film. The chromatographs resulting from automated sequencing of the 65 kDa band indicated that the first 10 amino acids at the N-terminus were AADAADDRPH. The two smaller bands (approximately 14 and 12 kDa) were sequenced to five amino acid residues, and the sequence AADAA was observed in each case. A sequence similarity search using the *fasta* program (Pearson and Lipman, 1988) identified the sequences as the major capsid protein, VP5, beginning at Ala791. This result is consistent with the appearance of two major bands at 85 and 65 kDa in the trypsin digestion experiments, because cleavage at Arg790 would produce fragments of roughly these sizes. The identified sequence is not found in any other HSV-1 capsid protein or in trypsin, suggesting that the 6F10 epitope is located within the carboxy-terminal domain of VP5, probably within 12–14 kDa of Ala791.

Recombinant GST–fusion proteins expressing segments of VP5 were created to more precisely map the epitope within the carboxy-terminus of VP5. Regions of the VP5 gene (UL19) corresponding to amino acids 1–790, 791–1374, 790–990, 790–890, 890–990, and 841–990 were subcloned into pGEX2T vector and transformed into bacteria. The ability of the plasmids to express recombinant fusion proteins was confirmed by SDS–PAGE analysis of whole cell lysates (Fig. 3a). Because the level of fusion protein expression appeared to be rather low for some of the larger constructs, particularly GEX2T (1–790) and GEX2T (791–1374), immunoblotting with polyclonal antiserum NC1, specific for VP5, was performed to verify that fusion proteins contained VP5 sequences (Fig. 3b). Both GEX2T (1–790) and GEX2T (791–1374) reacted strongly with the polyclonal antiserum, possibly because a greater proportion of the overall protein was present than in some of the smaller constructs, which displayed weaker reactivity. The empty pGEX2T vector was employed as a negative control and purified HSV-1 B-capsids provide a molecular weight standard and a positive control. A duplicate membrane was immunoblotted with mAb 6F10 (Fig. 3c), and a positive signal was observed only with proteins containing VP5 sequences

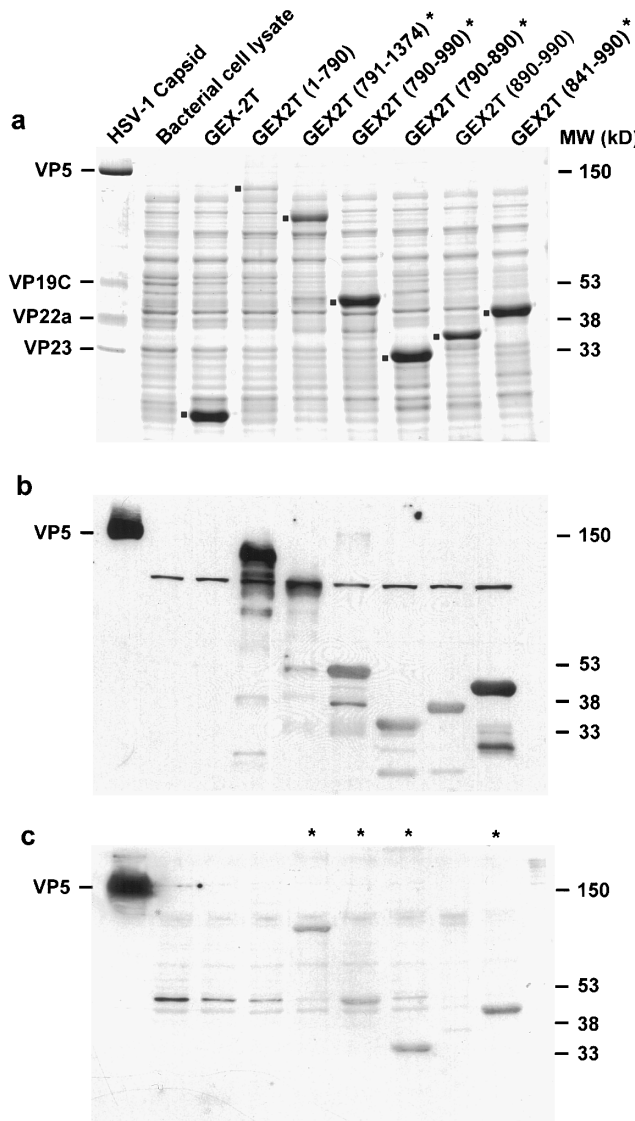

FIG. 3. SDS–PAGE and immunoblotting of GST-VP5 fusion proteins. Bacteria containing plasmids that expressed different GST-VP5 fusion proteins were induced as described in the text. Proteins from bacterial cell lysates were separated by electrophoresis on a 10% SDS–polyacrylamide gel and visualized by Coomassie staining (a). Fusion proteins (or GST alone) are indicated by a small dot. Duplicate gels were electrophoretically transferred to a nitrocellulose membrane and blotted with VP5-specific polyclonal antisera (b) or with mAb 6F10 (c). Asterisks indicate fusion proteins that react positively with mAb 6F10.

Dot Blot with mAb 6F10	Peptide	Sequence
	HSV-1 Capsid	Full length VP5
	790-808	RAADAADDRPHRGADWTVH
	805-823	WTVHHKIYYYVNPAFSRG
	819-837	AFSRGRCCTAGVRFDRVYA
	834-852	RYVATLQNMVVPEIAPGEE
	848-865	APGEECPSDPVTDPAHPL
	862-880	AHPLHPANVANTVNAMFH
	877-894	AMFHNGRVVVDGPAMLTL
	891-909	MLTLQVLAHNMAERTTALC

FIG. 4. Dot blot analysis of synthetic VP5 peptides. Peptides were adsorbed onto a nitrocellulose membrane and detected with mAb 6F10. For each peptide, the amino acid sequence and its position in the VP5 molecule are shown.

between Ala791 and the C-terminus. The fusion protein that contained only VP5 sequences from the amino-terminus to Arg790 did not react with mAb 6F10. The lanes containing GEX2T (791–1374), GEX2T (790–990), and GEX2T (790–890) are starred to indicate that these fusion proteins specifically reacted with mAb 6F10. The above results map the mAb 6F10 epitope to the region between amino acids 791 and 890. One additional construct, GEX2T (841–990) gave a positive signal when probed with mAb 6F10, further restricting the antibody binding site to amino acids 841–890 (Fig. 3c).

Synthetic peptides were utilized to define the specific amino acid residues recognized by mAb 6F10. Overlapping peptides were constructed to span the region from 790–909 of VP5. Figure 4 shows the sequence of each peptide beside the results of the dot blot. Only one peptide (862–880) reacted with mAb 6F10, mapping the 6F10 epitope to an 18 amino acid region in the central domain of VP5. The specificity of the reaction was confirmed by immunoblotting the same peptides with a VP22a-specific monoclonal antibody (MCA406), which reacted with only the B-capsid control (data not shown). Thus, the epitope of mAb 6F10 is believed to be contained within the peptide 862–880.

DISCUSSION

Cryoelectron microscopy and three-dimensional image analysis of antibody-labeled capsids showed that mAb 6F10 binds at the capsomer surface, near the *trans*-capsomeric channel (Fig. 1). Immunoblotting experiments mapped the epitope to the 18 amino acid peptide 862–880. Relating the structural information to the epitope reveals specific amino acid residues that are displayed at the capsomer surface. It is of note that recent studies of capsid assembly have identified a spherical capsid precursor, the procapsid, which is also recognized by mAb 6F10 (Newcomb *et al.,* 1996). Image reconstructions of the procapsid precipitated with mAb 6F10 showed that the antibody binds at the tips of the loosely formed hexons (Trus *et al.,* 1996). The structure of the mAb 6F10 epitope therefore appears to be conserved throughout capsid maturation, as well as through subsequent chemical manipulations of the capsid. In bacteriophage T4 maturation, some antibody epitopes were shown to switch between the inner and the outer capsid surfaces, while other epitopes remained in place (Steven *et al.,* 1991). Although major structural rearrangements do occur during HSV-1 procapsid maturation, they do not appear to affect either the integrity of the 6F10 epitope or its location at the outer tip of the protomer. In contrast, more significant conformation changes are expected in the portions of VP5 that form the capsid floor, which appears open and porous in the procapsid but smooth and continuous in the mature form (Newcomb *et al.,* 1996; Trus *et al.,* 1996).

The epitope identification methods described here have the potential to map the overall path followed by a polypeptide chain in a multiprotein complex. Although these techniques are most useful with antibody epitopes that are more linear in nature, conformational epitopes can still provide important structural information (Trus *et al.,* 1992). The X-ray crystallographic structure of SV40 capsid protein VP1 shows the C-terminal tail of each VP1 subunit extending into the adjacent capsomer while the N-terminal region reaches inside the capsid, possibly interacting with the viral DNA (Liddington *et al.,* 1991). Such a motif is conceivable for the HSV-1 major capsid protein VP5. The terminal regions of VP5 were unaffected by the proteolysis experiments described here, suggesting that trypsin was unable to access these regions or that they are in some way structurally protected from proteolytic digestion. In fact, it is possible that one or both of the terminal domains of VP5 may contain an eight-stranded anti-parallel β-barrel structure characteristic of many icosahedral plant and animal viruses, such as tomato busy stunt virus (Harrison *et al.,* 1978) and SV40 (Liddington *et al.,* 1991). In contrast, the central domain of the VP5 molecule was shown to be accessible to proteolytic digestion and to contain antigenic sequences, thus this domain must be highly exposed. Secondary structure modeling programs like the Chou–Fasman (Chou and Fasman, 1974) and Garnier–Robson (Garnier *et al.,* 1978) algorithms predict that the VP5 domain at the 6F10 epitope (862–880) may be a loop structure. Interestingly, in the coat protein of bacteriophage ϕX174, large insertion loops between regions of β-sheets have been implicated in protein–protein interactions (Ilag *et al.,* 1994; Fane and Hayashi, 1991). A second look at the sequence of VP5 in the HSV-1 capsid shows a region that is rich in proline residues near the exposed epitope site identified here (849-PEIAPGEECPSDPVTDPAHPLA-HPLHP-874). Proline-rich domains are common sites for

protein interactions and in particular the PXXP motif is a core consensus sequence for binding to SH3 domains (Cichetti *et al.,* 1992; Cohen *et al.,* 1995; Ren *et al.,* 1993). SH3 domains are found in many signalling and cytoskeletal proteins, making it attractive to speculate that the capsid may be involved in interactions with host cell proteins which facilitate signalling or trafficking. Further investigation in this area could reveal a novel mechanism for intracellular signalling or transport of viral pathogens.

ACKNOWLEDGMENTS

We thank Gary Cohen for providing polyclonal antiserum NC1, David Rekosh for supplying the pGEX2T vector, John Shannon for protein sequencing, Nathan Griggs for peptide synthesis, and Stephanie Gaillard for virus purification. We gratefully acknowledge grant support from the NSF (MCB-941770) and NIH (AI-137549).

REFERENCES

Baker, T. S., and Cheng, R. H. (1996). A model-based approach for determining orientations of biological macromolecules imaged by cryoelectron microscopy. *J. Struct. Biol.* 116 120–130.

Baker, T. S., Newcomb, W. W., Booy, F. P., Brown, J. C., and Steven, A. C. (1990). Three-dimensional structures of maturable and abortive capsids of equine herpesvirus 1 from cryoelectron microscopy. *J. Virol.* 64, 563–573.

Booy, F. P., Trus, B. L., Newcomb, W. W., Brown, J. C., Conway, J. F., and Steven, A. C. (1994). Finding a needle in a haystack: Detection of a small protein (the 12-kDa VP26) in a large complex (the 200 MDa capsid of the herpes simplex virus). *Proc. Natl. Acad. Sci. USA* 91, 5652–5656.

Chou, P. Y., and Fasman, G. D. (1974). Prediction of protein conformation. *Biochemistry* 13, 222–245.

Cicchetti, P., Mayer, B. J., Theil, G., and Baltimore, D. (1992). Identification of a protein that binds to the SH3 region of Abl and is similar to Bcr and GAP-rho. *Science* 257, 803–806.

Cohen, G. B., Ren, R., and Baltimore, D. (1995). Modular binding domains in signal transduction proteins. *Cell* 80, 237–248.

Fane, B. A., and Hayashi, M. (1991). Second-site suppressors of a cold sensitive prohead accessory protein of bacteriophage ϕX174. *Genetics* 128, 663–671.

Francis, N. R., Irikura, V. M., Yamaguchi, S., DeRosier, D. J., and Macnab, R. M. (1992). Localization of the *Salmonella typhimurium* flagellar switch protein FliG to the cyroplasmic M-ring face of the basal body. *Proc. Natl. Acad. Sci. USA* 89, 6304–6308.

Garnier, J., Osguthorpe, D. J., and Robson, B. (1978). Analysis of the accuracy and implications of a simple method for predicting the secondary structure of globular proteins. *J. Mol. Biol.* 120, 97–120.

Gibson, W., and Roizman, B. (1972). Proteins specified by herpes simplex virus. VIII. Characterization and composition of multiple capsid forms of subtypes 1 and 2. *J. Virol.* 10, 1044–1052.

Harrison, S. C., Olson, A. J., Schutt, C. E., Winkler, F. K., and Bricogne, G. (1978). Tomato bushy stunt virus at 2.9 A resolution. *Nature* 276, 368–373.

Ilag, L. L., McKenna, R., Yadav, M. P., BeMiller, J. N., Incardonna, N. L., and Rossman, M. G. (1994). Calcium induced structural changes in bacteriophage ϕX174. *J. Mol. Biol.* 244, 291–300.

Liddington, R. C., Yan, Y., Moulai, J., Sahli, R., Benjamin, T. L., and Harrison, S. C. (1991). Structure of simian virus 40 at 3.8-A resolution. *Nature* 354, 278–284.

Newcomb, W. W., Homa, F. L., Thomsen, D. R., Booy, F. P., Trus, B. L., Steven, A. C., Spencer, J. V., and Brown, J. C. (1996). Assembly of the herpes simplex virus capsid: Identification of intermediates in cell-free capsid formation. *J. Mol. Biol.* 263, 432–446.

Newcomb, W. W., Trus, B. L., Booy, F. P., Steven, A. C., Wall, J. S., and Brown, J. C. (1993). Structure of the herpes simplex virus capsid: Molecular composition of the pentons and the triplexes. *J. Mol. Biol.* 232, 499–511.

Newcomb, W. W., and Brown, J. C. (1991). Structure of the herpes simplex virus capsid: Effects of extraction with guanidine hydrochloride and partial reconstitution of extracted capsids. *J. Virol.* 65, 613–620.

Olson, H. M., Nag, B., Etchison, J. R., Traut, R. R., and Glitz, D. G. (1991). Differential localization of two epitopes of *Escherichia coli* ribosomal protein L2 on the large ribosomal subunit by immune electron microscopy using monoclonal antibodies. *J. Biol. Chem.* 166, 1898–1902.

Pearson, W. R., and Lipman, D. J. (1988). Improved tools for biological sequence comparison. *Proc. Natl. Acad. Sci. USA* 85, 2444–8.

Perdue, M. L., Cohen, J. C., Kemp, M. C., Randall, C. C., and O'Callaghan, D. J. (1975.) Characterization of three species of nucleocapsids of equine herpes virus type 1. *Virology* 64, 187–205.

Ren, R., Mayer, B. J., Cicchetti, P., and Baltimore, D. (1993). Identification of a ten-amino acid proline-rich SH3 binding site. *Science* 259, 1157–1161.

Roizman, B. (1996). Herpesviridae: A brief introduction. *In* "Virology" (B. N. Fields, D. M. Knipe, P. M. Howley, R. M. Chanock, J. L. Melnick, T. P. Monath, S. E. Strauss and B. Roizman, Eds.), 3rd ed., pp. 2231–2295. Lippincot-Raven, Philadelphia.

Schrag, J. D., Prasad, B. V. V., Rixon, F. J., and Chiu, W. (1989). Three-dimensional structure of the HSV1 nucleocapsid. *Cell* 56, 651–660.

Smith, T. J., Olson, N. H., Cheng, R. H., Chase, E. S., and Baker, T. S. (1993). Structure of a human rhinovirus-bivalently bound antibody complex: Implication for viral neutralization and antibody flexibility. *Proc. Natl. Acad Sci. USA* 90, 7015–7018.

Steven, A. C., Bauer, A. C., Bisher, M. E., Robey, F. A., and Black, L. W. (1991). The maturation-dependent conformational change of phage T4 capsid involves the translocation of specific epitopes between the inner and the outer capsid surfaces. *J. Struct. Biol.* 106, 221–236.

Steven, A. C., Roberts, C. R., Hay, J., Bisher, M. E., Pun, M., and Trus, B. L. (1986). Hexavalent capsomers of herpes simplex virus type 2: symmetry, shape, dimensions and oligomeric status. *J. Virol.* 57, 578–584.

Trus, B. L., Booy, F. P., Newcomb, W. W., Brown, J. C., Homa, F. L., Thomsen, D. R., and Steven, A. C. (1996). The herpes simplex virus procapsid: structure, conformational changes upon maturation, and roles of the triplex proteins VP19c and VP23 in assembly. *J. Mol. Biol.* 263, 447–462.

Trus, B. L., Homa, F. L., Booy, F. P., Newcomb, W. W., Thomsen, D. R., Cheng, N., Brown, J. C., and Steven, A. C. (1995). Herpes simplex virus capsids assembled in insect cells infected with recombinant baculoviruses: Structural authenticity and localization of VP26. *J. Virol.* 69, 7362–7366.

Trus, B. L., Newcomb, W. W., Booy, F. P., Brown, J. C., and Steven, A. C. (1992). Distinct monoclonal antibodies separately label the hexons or the pentons of herpes simplex virus capsid. *Proc. Natl. Acad. Sci. USA* 89, 11508–11512.

Zhou, Z. H., He, J., Jakana, J., Tatman, J. D., Rixon, F. J., and Chiu, W. (1995). Assembly of VP26 in herpes simplex virus-1 inferred from structures of wild-type and recombinant capsids. *Nature Struct. Biol.* 2, 1026–1030.

Zhou, Z. H., Prasad, B. V. V., Jakana, J., Rixon, F. J., and Chiu, W. (1994). Protein subunit structures in the herpes simplex virus A-capsid determined from 400kV spot-scan electron cryomicroscopy. *J. Mol. Biol.* 242, 456–469.